P5M.3

MAINTENANCE OF A MOUNTAIN VALLEY COLD POOL: A NUMERICAL STUDY

Brian J. Billings*, Vanda Grubišić, and Randolph D. Borys
Desert Research Institute, Reno, NV

1. INTRODUCTION

Whiteman et al. (2001) define two types of cold pools. A diurnal cold pool forms during the evening or night and decays following sunrise the next day. A persistent cold pool lasts longer than one diurnal cycle. Therefore, a cold pool that survives the solar heating of the daylight hours is a persistent one. Persistent cold pools can have significant effects on human activities (Whiteman et al. 1999). Air pollution can accumulate to unacceptably high levels, liquid precipitation falling into the cold pool can produce freezing rain or drizzle, and cold pools can delay the melting of snow and the breakup of ice on rivers. Despite their significant impact, forecasting the buildup and removal of persistent cold pools remains a challenging problem (Zhong et al. 2001).

The temperature inversion associated with a valley cold pool may not extend to the top of the surrounding ridges. This will result in a band of relatively warmer temperatures known as a thermal belt (Geiger et al. 1995) partway up the sidewalls. Since a thermal belt can be identified in the surface temperatures ascending the valley slopes, cold air pooling can be identified even in upper-air measurements are unavailable, as is the case for this study.

In this study, we investigate a persistent cold pool and thermal belt that affected the Yampa Valley of Colorado throughout 10 January 2004. The purpose of this study is to assess the importance of various factors on numerical model simulations of the cold pool. These simulations are compared to observations that were taken during a field research course in the Yampa Valley.

2. METHODOLOGY

2.1 *Topography, Observing Sites, and Dataset*

The upper Yampa Valley (south of Steamboat Springs, CO) is a roughly north-south oriented valley that cuts through the western slope of the Rocky Mountains for a distance of approximately 70 km (Fig. 1). The valley floor has a width of approximately 3.5 km just south of Steamboat Springs, while the ridge to ridge distance is approximately 11 km. The valley floor lies at an average elevation of 2050 m MSL and rises to average elevations of 2400 m MSL on its western side and over 3000 m MSL on its eastern side. At the top of the eastern summit, at an elevation of 3210 m MSL is the Desert Research Institute's (DRI) Storm Peak Laboratory (SPL; Borys and Wetzel 1997), which serves as the operations center for a field research course offered by the University of Nevada-Reno and the DRI.

The observational network for this study consists of a line of automated surface stations on the eastern slope of the valley. All stations report temperature and relative humidity, but only stations at higher elevations report wind data. Additionally, none of the stations report pressure, so the potential temperature cannot be calculated. The temperature sensors have a range of -40°C to +60°C and are accurate to $\pm$0.3°C at 0°C. The stations used in this dataset follow a relatively straight path up the valley sidewall.

2.2 *Synoptic Overview*

Data collection at Storm Peak Laboratory began on 5 January 2004 (the dates in this section correspond to LST), shortly after the passage of a large 500 hPa trough, which had generated a significant amount of snowfall over the area. On 6-7 January, the flow became more zonal, and a pair of minor shortwaves moved through, creating overcast skies and additional snowfall. On 8 January, flow turned to the northwest as a ridge began to build in from the south. This ridge reached a maximum amplitude on 9 January, as a closed high moved into Arizona. The high continued north into the Four Corners region on 10 January.

While the ridge of 8-10 January cleared skies in many areas, in certain regions the stagnant flow and recent snowfall led to widespread dense fog. Mount Werner (Fig. 1) remained enveloped in cloud until clearing occurred during the afternoon and evening of 9 January. At areas further down the slope, the fog dissipated on the afternoon of 8 January, but in the lowest portion of the valley, fog redeveloped during the evenings of 8 and 9 January. This fog dissipated shortly after sunrise on 10 January, and the rest of the day was mostly clear, with the exception of significant contrail activity in the morning that lasted approximately 90 minutes. An inversion formed in the valley shortly after sunset on 8 January. Despite clearer skies, the cold pool survived each diurnal cycle for at least four more days, at which time measurements were no longer saved. The choice was made to simulate this cold pool for one diurnal cycle, that of 10 January 2004.

2.3 *Model Description*

The model used in this study was the Pennsylvania State University-National Center for Atmospheric Research Mesoscale Model version 5 (MM5; Grell et al. 1994). The baseline simulations contained four nested two-way interactive domains, all roughly centered

*Corresponding author address: Brian J. Billings, Division of Atmospheric Sciences, Desert Research Institute, Reno, NV 89512; e-mail: billings@dri.edu

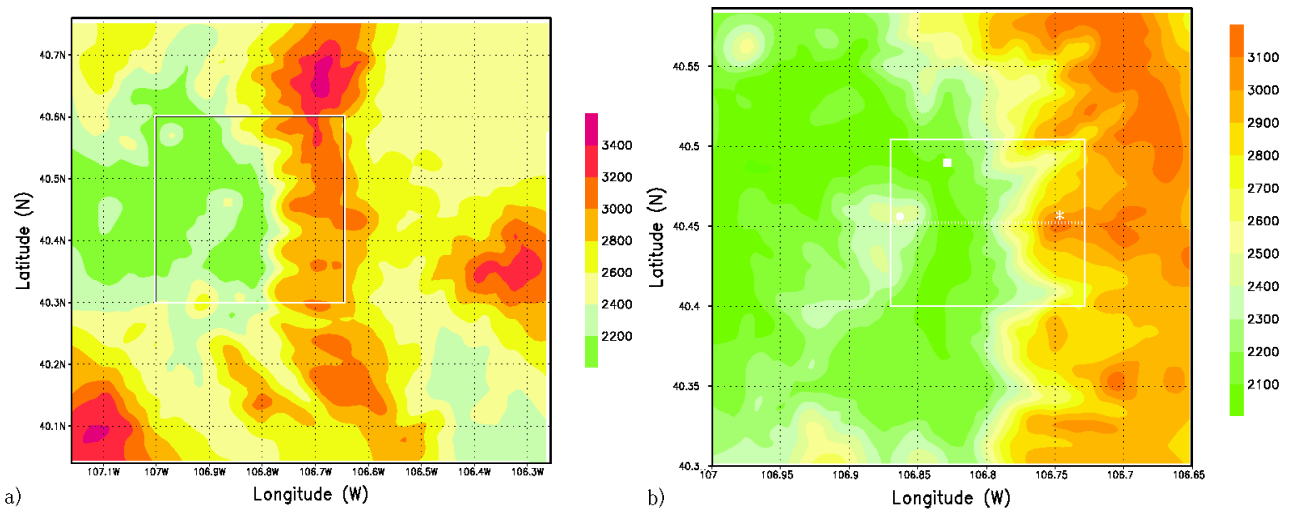

FIG. 1: (a) Topography of the upper Yampa Valley from the 1 km domain. Contours are shown every 200 m. (b) Topography of the upper Yampa Valley from the 333 m domain. Contours are shown every 100 m. Marked are the locations of the model cross section (thick solid line), Mount Werner and Storm Peak Laboratory (asterisk), Quarry Mountain (circle), and Steamboat Springs (square).

over the field site, with resolutions of 27, 9, 3, and 1 km. All of the nests were run for the entire length of the simulation. In the vertical, fifty-one sigma levels were used, with finer resolution in the lowest levels of the atmosphere corresponding to approximately 20 m. Terrain elevation, land-water mask, and vegetation data were taken from the U.S. Geological Survey dataset of the corresponding resolutions. Initial and boundary conditions, including snow cover analysis, were provided by the National Center for Environmental Prediction Global Forecast System (GFS) model reanalyses, with a horizontal resolution roughly equivalent to 55 km. All of the runs used the MM5's Grell cumulus parameterization, Dudhia simple ice microphysical scheme, and cloud-radiation scheme.

The time period for the baseline model simulations was 1200 UTC (0500 LST) 10 January 2004 to 0000 UTC 11 January (1700 LST 10 January) 2004. (The model was initialized with the GFS reanalyses at the start of this baseline period.) The evolution of inversion breakups studied by Whiteman (1982) depended on snow cover and the growth of a convective boundary layer. Therefore, two parameters were varied in the baseline simulations: 1) the use of snow cover analysis and 2) the planetary boundary layer (PBL) parameterization. Based on the results of these simulations, additional sensitivity runs were performed, in which the following parameters were changed: 1) the vertical resolution, 2) the model start time, 3) the horizontal resolution, and 4) the horizontal diffusion scheme.

3. RESULTS

Figure 2 shows the evolution of the temperature profile across the valley from before sunrise to after sunset on 10 January for the baseline simulation. The observations clearly defined a thermal belt located midway up the valley's eastern slope. This feature remains in place throughout the day, while the temperatures rise significantly, except for the station near the summit. Three hours into the model simulation, there is a temperature maximum at the same elevation as seen in the observations and a relative minimum at the valley floor (Fig. 2a). The simulated temperatures above the inversion matched the observations well, but the temperatures within the cold pool were not as cold as was observed.

After sunrise, the model solution quickly diverges from the observations. Three hours later (Fig. 2b), the temperature in the valley is nearly isothermal at the approximate melting point for ice. Near the warmest part of the day, the simulated temperature profile displays the typical decrease in temperature with elevation (Fig. 2c). After sunset, the valley is again nearly isothermal, though a new inversion is beginning to form (Fig. 2d).

The previous simulation setup was performed with and without snow cover for five of the MM5's seven available PBL parameterizations (excluding the simplified bulk PBL and computationally expensive high-resolution Blackadar PBL scheme): the Burk-Thompson PBL, the Eta PBL, the MRF PBL, the Gayno-Seaman PBL, and the Pleim-Chang PBL. For the same snow cover analysis, similar results were obtained for almost all of the PBL schemes. (The one exception will be discussed in the following subsection.) The average temperature varied slightly between the schemes, but all of the parameterizations resulted in nearly identical temperature structures, transitioning from a weak thermal belt through an isothermal pattern to a temperature maximum on the valley floor. For this reason, only one PBL scheme (MRF) was used for the remainder of the study.

Since the baseline simulations were unable to maintain a cold pool in the valley throughout the day, additional simulations were performed in an effort to improve the

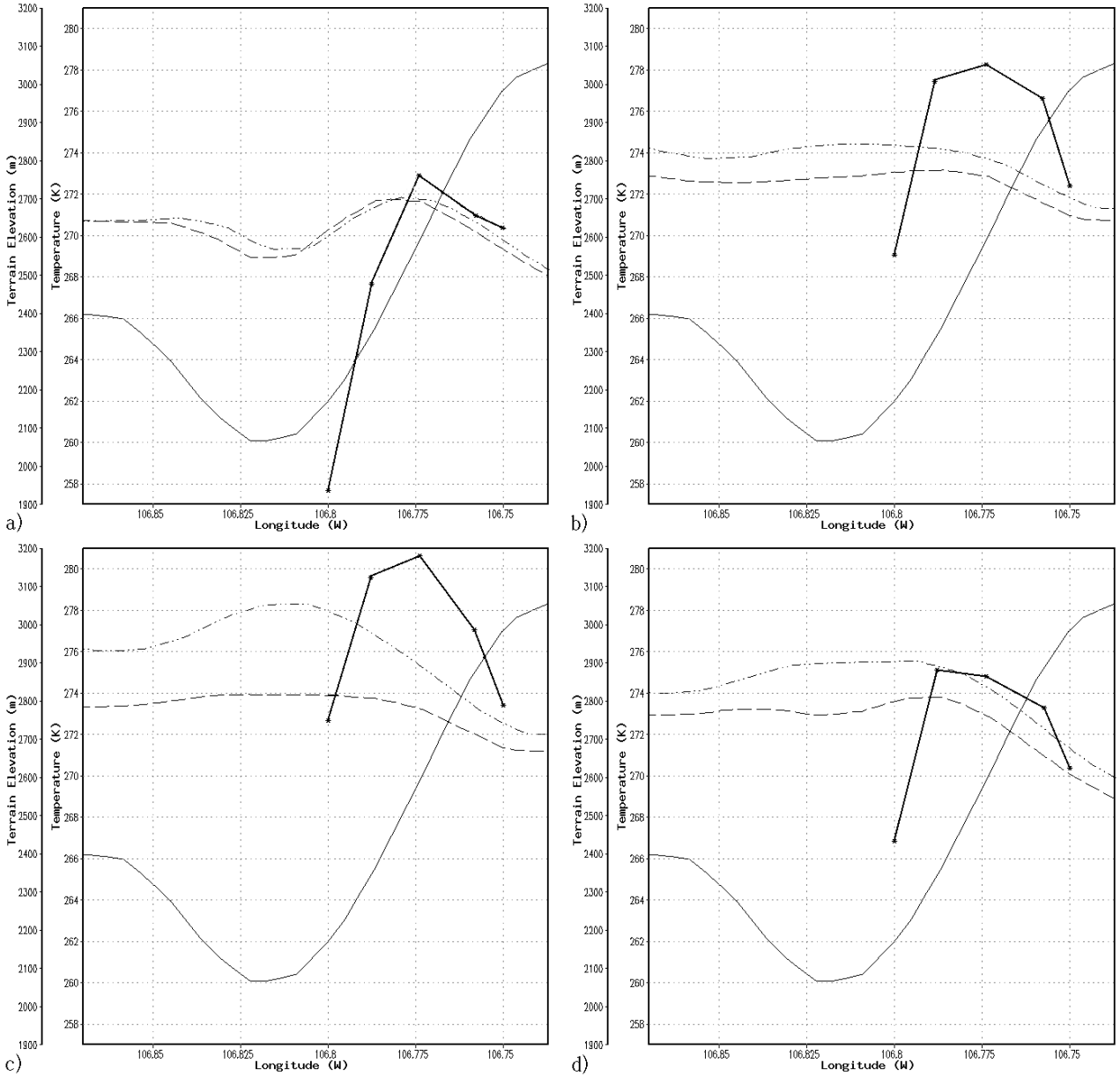

FIG. 2: Cross-section of the terrain height (thin solid line), observed temperature (thick solid line), and model simulated temperature for 1 km resolution with snow cover (dashed line) and without snow cover (dot-dashed line) along the lowest sigma surface for (a) 15 UTC (08 LST), (b) 18 UTC (11 LST), and (c) 21 UTC (14 LST) 10 January and (d) 00 UTC 11 January (17 LST 10 January) 2004.

model forecast. First, the number of vertical levels was increased form 51 to 100 levels, resulting in approximately 10 m resolution in the lower levels. This did not result in a significant change in the model simulation and the cold pool maintenance. Then, using the same increased vertical resolution, the model was started 12 hours earlier, at 00 UTC 10 January 2004, so that the model physics had additional time to spinup. As with the higher vertical resolution, the additional spinup time did not significantly change the results of the baseline simulations, particularly during the daylight hours when the isothermal profile dominated the valley. The 00 UTC start time was retained to provide additional data for analysis.

3.1 *Snow Cover Effects*

The persistent cold pools observed by Whiteman (1982) occurred in the presence of snow cover. To determine the importance of this effect, additional simulations were run without snow cover for all five PBL parameterizations. Figure 2 shows the 24-hour temperature profile evolution for the 1 km run with and without snow cover analysis. In the absence of snow cover, the results begin to differ significantly once solar radiation commences. While the simulation with snow cover mainly produces an isothermal temperature profile across the valley, the simulation without snow cover contains an exaggerated dependence of temperature on elevation, such that there is a very distinct maximum at the valley floor and minimas on either summit. While the simulation with snow cover was not successful, its isothermal lapse rate is closer to reality than the simulation which did not use snow cover. The primary effect of snow cover appears to be an increased albedo. In the presence of snow cover, there is far more reflected solar radiation, resulting in a lower sensible heat flux, particularly at the lowest three stations, leading to a closer representation of the cold pool.

Four of the five PBL paramterizations resulted in nearly the same variation when the snow cover was not included in the simulation set up. However, the Pleim-Chang PBL resulted in similar, though not identical, temperature profiles. This PBL scheme is a combined land-surface and PBL model; therefore, it uses a different surface scheme than the other PBL parameterizations in this study. It appears that due to a simple treatment of snow cover in the Pleim-Xiu land surface model, when temperatures are below freezing the snow cover has much less effect (J. E. Pleim 2004, personal communication).

3.2 *Horizontal Resolution Effects*

The next factor that was modified was the horizontal resolution. First, a 333 m domain was nested inside the fourth domain of the previous model setup. The finest horizontal resolution that could be achieved with a reasonable computation time was 111 m. Both sub-kilometer resolutions produced generally similar results. Figure 3 shows the results for the 111 m resolution simulation throughout the daytime of 10 January. During the first two time periods, before sunrise, there is a very distinct cold pool in the model simulation that matches the observations relatively well with the exception of the minimum temperature in the valley (Fig. 3a). At 1800 UTC (1100 LST), the temperature inversion has started to erode and the magnitude of the cold pool has lessened (Fig. 3b). This is also the time when the mid-slope mesonet stations begin to warm much faster than in the model simulation. Near the warmest part of the day, the temperature structure is similar to the results of the 333 m run, with a very weak cold pool and thermal belt still in the valley (Fig. 3c). At the final time period, after sunset, the cold pool has started to strengthen again, and the model simulations are again in relatively good agreement with the observations (Fig. 3d).

In the 1 km simulation, the thermal belt is defined by only 5 horizontal grid points. However, when the horizontal resolution is tripled, the observational area is now spanned by 15 grid points and feature resolution is much improved. Similarly, the 20 m vertical resolution was adequate for feature resolution, which explains why doubling the vertical resolution did not significantly improve the forecast. Additional analysis reveals more mechanisms for improvement of the simulation due to finer resolution.

Both sub-kilometer resolution runs produce generally similar results, even though in the 333 m simulation, drainage flows evacuate air from the valley, with little or no inflow from any source, whereas when the horizontal resolution is increased to 111 m, there is a significant change in the valley circulation. With air near the ends of the valley still flowing out through passes to the east, in the center of the valley, a large eddy formed which kept the air circulating in the valley instead of draining out. While Zängl (2003) showed that drainage flows can cause cold pools in open valleys to disappear more quickly than in closed basins, the wind speed in both cases is on the order of 1-2 m s^{-1}, so these different circulation patterns do not significantly affect the results of the simulation. In the case of stronger wind speeds, this would be an important mechanism in cold pool retention.

Increased resolution also affects the energy budget, by means of a more precise land use analysis. In the 1 km analysis, the lowest mesonet station is located in an area of tundra. However, in the 111 m analysis, this station is in an area of wet or marsh land. Conversely, the 111 m analysis locates the highest station in the tundra category, while in the 1 km simulation, this station is located in an agriculture land use category. Since the tundra land use category has one of the highest moisture availabilities in the MM5, these differences result in a lower latent heat flux at the bottom station and a higher flux at the top in the finer resolution simulations.

3.3 *Horizontal Diffusion Effects*

In MM5, horizontal diffusion is calculated along the model's terrain-following sigma-coordinate surfaces. Adjacent grid points on the same sigma surface lie at significantly different elevations and have significantly different temperatures, resulting in overactive horizontal diffusion. Increasing the horizontal resolution will reduce this effect, but Zängl (2002) demonstrates a less expensive way to correct for these numerical errors by calculating the truly horizontal diffusion on a constant height level.

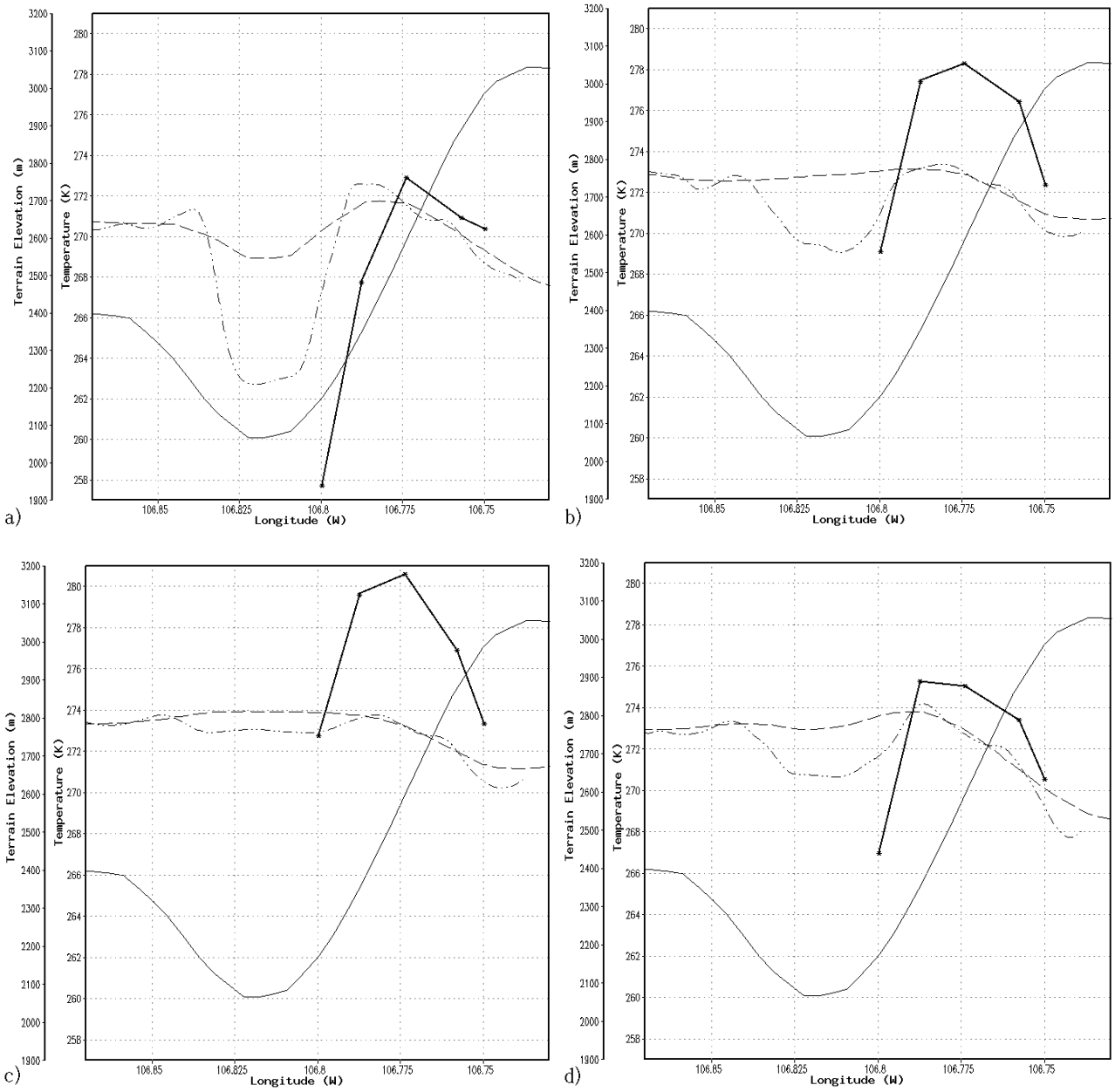

FIG. 3: Cross-section of model simulated temperature for 1 km resolution (dashed line) and 111 m resolution (dot-dashed line). Terrain, observed temperature, and times are the same as Fig. 2.

This horizontal diffusion method has been made available in the latest version of the MM5. Consequently, the Yampa Valley cold pool was simulated again at 1 km and 111 m resolution, using the Zängl (2002) horizontal diffusion scheme.

Figure 4 compares the evolution of the temperature structure in the valley using the Zängl diffusion scheme with the previous 1 km simulation. Just prior to sunrise (Fig. 4a), the true horizontal diffusion scheme has a better simulated cold pool in the valley. Not only is the temperature difference between the valley floor and mid-slope greater (in accordance with the observations), but also the maximum of the thermal belt is located further up the slope, indicating a deeper cold pool, which is again in a better agreement with the observations. As solar radiation begins (Fig. 4b), the simulation with the Zängl (2002) diffusion scheme is again not able to match the rapidly increasing observed temperatures, but a far more significant thermal belt is maintained as compared to the previous 1 km simulation. At the warmest part of the day (Fig. 4c), the truly horizontal diffusing scheme has maintained a very weak thermal belt, which did not occur in the previous simulations. After sunset (Fig. 4d), the simulated cold pool begins to restrengthen, with the maximum of the thermal belt located further downslope. This behavior is also seen in the mesonet observations. While decreasing the resolution to 111 m with the Zängl (2002) diffusion scheme did improve the simulation of inversion strength and sharpness, the improvements were not as dramatic as in the case of sigma diffusion.

4. CONCLUSIONS

A very persistent cold pool was observed in the upper Yampa Valley of northwester Colorado. This cold pool was simulated during one diurnal cycle. A baseline simulation did not match the strength of the observed inversion and did not retain it throughout the day. Varying the planetary boundary layer parameterization, doubling the vertical resolution, and starting the model 12 hours earlier did not significantly improve the results. A stronger inversion and maintenance throughout the day was obtained by i) the use of snow cover data, ii) increasing the horizontal resolution, and iii) computing the horizontal diffusion on constant height surfaces. Increased horizontal resolution improved the simulation by not only providing a sufficient number of grid points for feature resolution, but by resolving an airflow with less drainage out of the valley and providing a more accurate analysis of land use, which affected the latent heat flux. Computing the horizontal diffusion on constant height surfaces also allowed the cold pool to be retained.

The results of this study illustrate the often cited need for accurate snow cover analyses for initialization of operational weather models. In addition, the very high horizontal resolutions used in this study are not likely feasible for operational use in the near future, even for localized simulations run at regional forecast offices or universities. One solution is to implement a truly horizontal diffusion scheme to eliminate the errors caused by vertical gradients along sigma surfaces. However, due to the additional impacts of decreased horizontal resolution, it remains a responsibility of the local forecaster to understand how larger scale conditions will be manifest in small valleys which are difficult to resolve.

All of the simulations with snow cover do not seem capable of exceeding the melting point temperature. More experimentation with the MM5's surface schemes and their representation of snow cover may yield a more accurate result. Studying the entire life cycle of the cold pool would also be beneficial. Finally, future field programs with more extensive observations, such as tethersondes or additional surface wind observations, would provide more detailed information on the structure of the cold pools in this valley.

ACKNOWLEDGMENTS

The MM5 runs were performed on the SGI Altix of the Nevada Environmental Computing Grid (NECG) and on the Mesoscale Dynamics and Modeling Laboratory's 68-processor Sierra Cluster, both at DRI. NECG is part of the ACES program (http://www.aces.dri.edu), which is funded by NSF EPSCoR. The Sierra Cluster was funded by the NSF grant ATM-0116666. This research was supported in part by NSF grant ATM-0242886.

REFERENCES

Borys, R. D., and M. A. Wetzel, 1997: Storm Peak Laboratory: A research, teaching, and service facility for the atmospheric sciences. *Bull. Amer. Meteor. Soc.,* **78,** 2115-2123.

Grell, F. A., J. Dudhia, and D. R. Stauffer, 1994: A description of the fifth-generation Penn State/NCAR Mesoscale Model (MM5). NCAR tech. note, NCAR/TN-398 + STR, 122 pp. [Available from NCAR, P.O. Box 3000, Boulder, CO 80307.]

Whiteman, C. D., X. Bian, and S. Zhong, 1999: Wintertime evolution of the temperature inversion in the Colorado Plateau Basin. *J. Appl. Meteor.,* **38,** 1103-1117.

——, S. Zhong, W. J. Shaw, J. M. Hubbe, X. Bian, and J. Mittelstadt, 2001: Cold pools in the Columbia Basin. *Wea. Forecasting,* **16,** 432-447.

Zängl, G., 2002: An improved method for computing horizontal diffusion in a sigma-coordinate model and its application to simulations over mountainous topography. *Mon. Wea. Rev.,* **130,** 1423-1432.

——, 2003: The impact of upstream blocking, drainage flow, and the geostrophic pressure gradient on the persistence of cold-air pools. *Quart. J. Roy. Meteor. Soc.,* **129,** 117-137.

Zhong, S., C. D. Whiteman, X. Bian, W. J. Shaw, and J. M. Hubbe, 2001: Meteorological processes affecting the evolution of a wintertime cold air pool in the Columbia Basin. *Mon. Wea. Rev.,* **129,** 2600-2613.

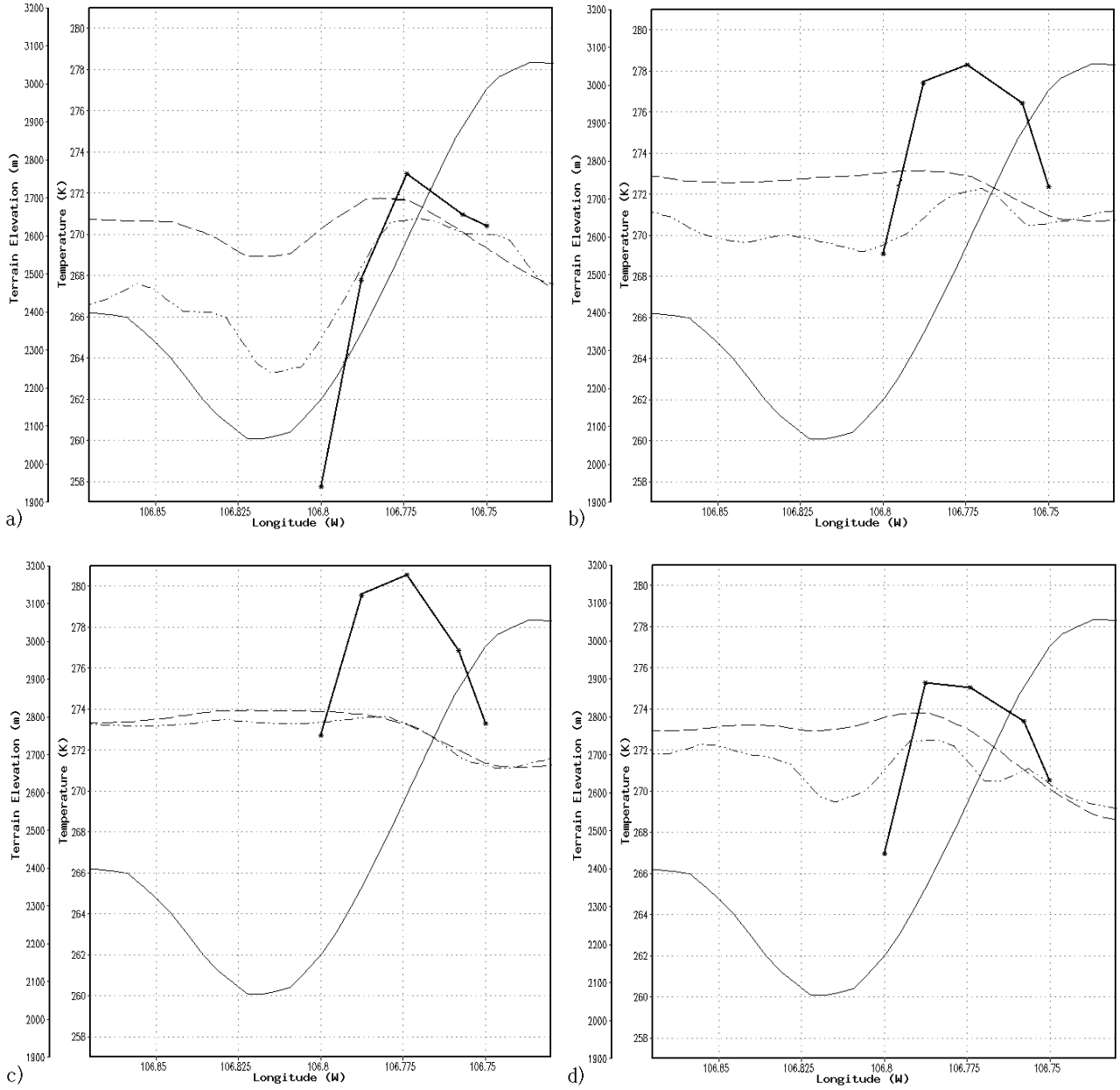

FIG. 4: Cross-section of model simulated temperature at 1 km resolution for sigma-coordinate diffusion scheme (dashed line) and Zängl diffusion scheme (dot-dashed line). Terrain, observed temperatures, and times are the same as in Fig. 2.